

Multistage Stirling Cycle Refrigeration Performance Mapping of the Ball SB235 Cryocooler

T. Roberts and A. Razani

Air Force Research Laboratory AFRL/VSSS
Kirtland AFB, NM 87117

ABSTRACT

The performance mapping of a multistage Stirling cycle refrigeration system has been performed on the Ball Aerospace SB235 cryocooler by the Air Force Research Laboratory. The results are presented in terms of primitive variables such as temperature, work inputs, and cooling load supported. It is then restated in terms of composite variables such as available work (exergy) inputs, the individual and composite exergies of the cooling loads supported, and system efficiency. The results of this mapping when stated in terms of these composite variables shows that overall cooling performance follows discernible, distinct paths as external environmental conditions such as work input, rejection temperature, or imposed cooling load change. This composite performance is analogous to how cooling performance of a real single stage refrigerator is determined by its functional performance manifold with respect to these same environmental variables. Further analysis of this performance of the SB235 cryocooler suggests theoretical approaches to the question of how multistage Stirling refrigeration systems proportion available work to the discrete stages as a function of cooling load temperature, total available work input to the system, and rejection temperature. The data provided by this mapping would therefore form the basis for a theoretical first order model of how practical application environments alter the relative refrigeration performances of multistaged cold ends which now has to be empirically measured or predictively modeled using high order composite component models.

INTRODUCTION

The widespread introduction of space flight quality cryogenic refrigerators into the trade space for a variety of missions has brought increased interest into designs which can support diverse cooling loads at different payload temperatures. These might include distinct loads at several focal plane arrays, the optics benches for these arrays, communication lasers, and other future uses which are common in terrestrial applications but which have been ignored by payload designers. The description of the performance of these devices has been a significant problem to date, as their thermodynamic output is delivered at these diverse stages.

EXERGETIC COOLING AND AVAILABLE WORK

It is a fairly common concept that due to energy conservation, any closed system's inputs, available work, must equal its outputs plus irreversibilities. What is not immediately obvious are the following empirical observations, given the same set of equilibrium inputs, environmental conditions and loads:

1. Any stable refrigerator will deliver the same outputs over time.
2. The ratio of the cooling loads in a multistage cooler is invariant.

The rationale for the first observation hinges upon the system of parabolic partial differential equations which describe the operation of the cryogenic refrigeration system where various heat and momentum transfer phenomena diffuse and damp the acoustic phenomena leading to refrigeration in Stirling variants or any flow instabilities in reverse Brayton or Joule-Thomson devices. Explaining why observation 2 should be true is the subject of this study, for there is no a priori reason based upon a system level. Instead, an explanation must rest on how the system operation interacts with component level phenomena which are not obvious or measurable by external transducers.

In order to provide a common basis for such external measurements of performance, the following definitions of exergetic cooling and exergetic efficiency (otherwise known as fraction of Second Law Limit) are provided:

$$Q_{cooling,exer} = \sum_{i=1}^n Q_i \left(\frac{T_{rej}}{T_{cooling,i}} - 1 \right) \quad (1)$$

$$\eta_{exer} = \frac{Q_{cooling,exerg}}{P_{input}} \quad (2)$$

SB235 COOLING PERFORMANCE MEASUREMENTS

This split Stirling refrigerator was instrumented with the conventional silicon diode cryogenic thermometry transducers for all temperature measurements below 150 K, and thermocouples for other temperature measurements. A Valhalla 2100™ Series Benchtop Power Analyzers measured both power to the compressors, the expander motor, and the balancer. The cooling performance description of this refrigerator can be described as shown in Figures 1 through 4. This methodology is unappealing for several reasons:

1. Unless a specific stage load is specified and becomes invariant in such a study, the number of data points needed to compile a full set of descriptive graphics such as Figures 1 through 3 becomes too costly to characterize for the complete performance envelope of a two stage cooler.
2. Figure 4 alludes to a possible method for consolidating results, but like Figures 1 through 3 it presumes that the need is solely for performance at discrete power inputs or strokes and rejection temperatures, whereas real systems operate smoothly within their operation envelopes.
3. Attempts to mathematically estimate these performance manifolds are singularly unproductive due to the fact that they depict many interrelated, nonlinear phenomena which are presently poorly understood.

It is asserted at this point that resolving the issues of the first two points must address the deficiency of the third point.

Figures 1 through 3 allude to a phenomena which will be of great interest in the rest of this article: as the low stage load increases, the temperature of the higher stage flattens and then slightly *decreases*. In exergetic cooling terms, the proportion of exergetic cooling between the stages is shifting, as shown in Figure 5. This furthermore implies that the proportion of available work being used to produce refrigeration in these two stages changes. The overall efficiency of the refrigerator is related to the sum of the efficiencies of its stages, so this in turn implies that if a stage would optimally run at a certain temperature, then if it is loaded so that it will either run lower or high, then its efficiency will decline. This reduction in stage efficiency might be ameliorated by a transfer of exergetic cooling load to another stage, if that stage is becoming more efficient. Conversely, the

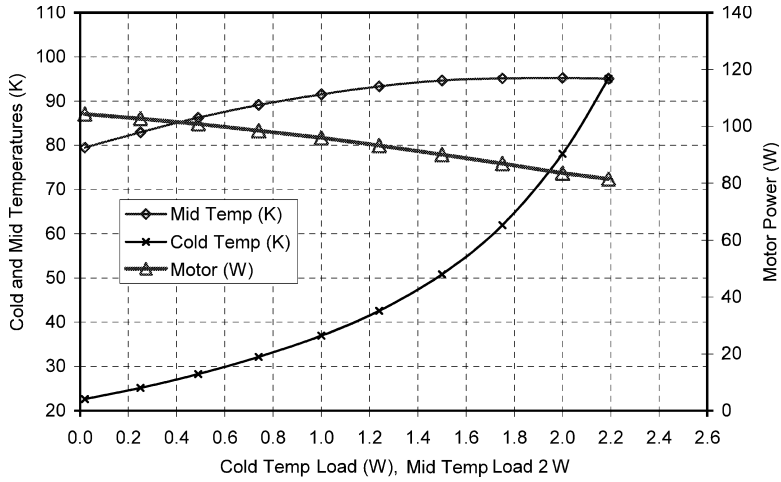


Figure 1. Performance at 275 K rejection, 85% stroke.

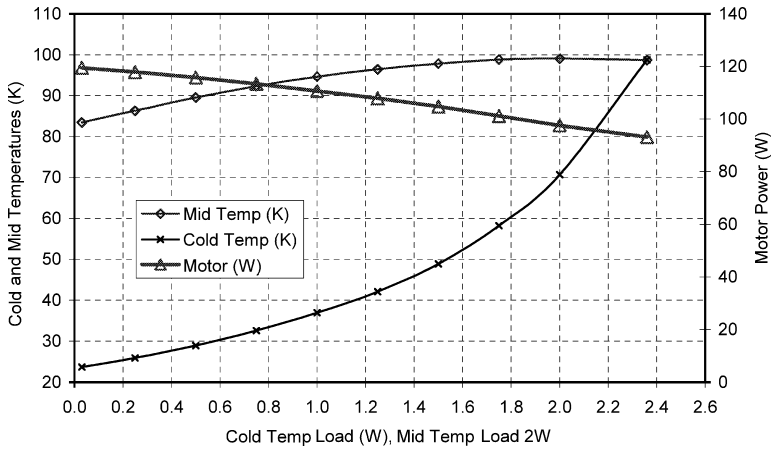


Figure 2. Performance at 300 K rejection, 85% stroke.

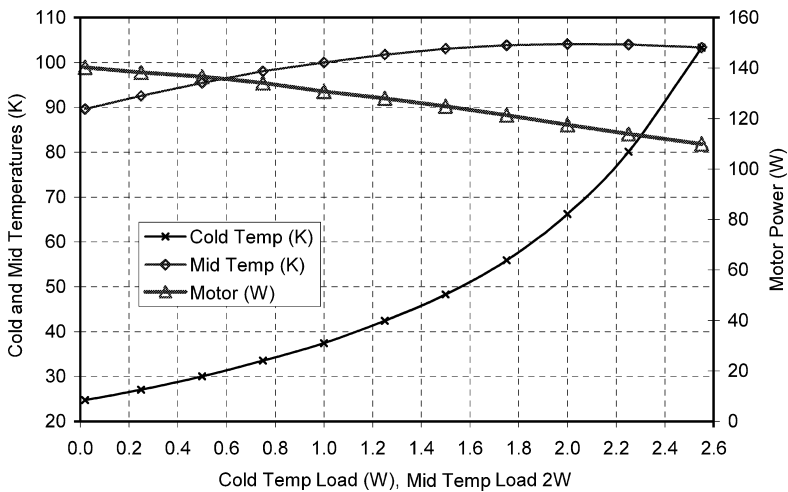


Figure 3. Performance at 320 K rejection, 85% stroke.

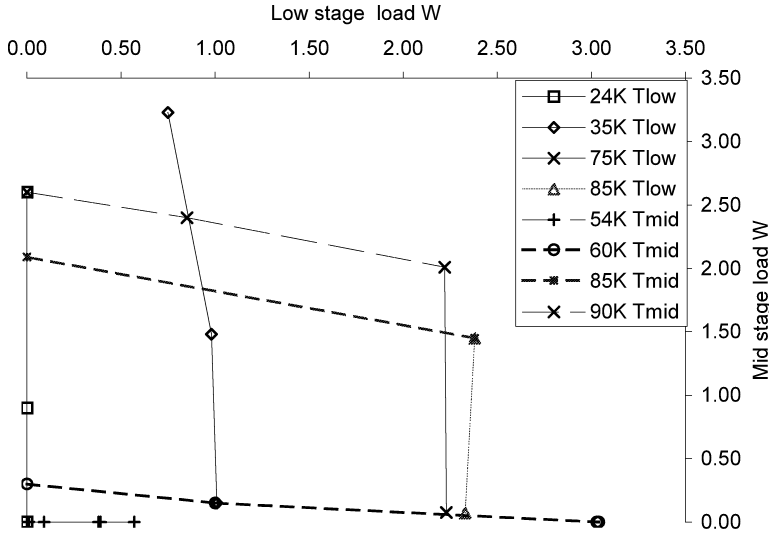


Figure 4. Performance at 300 K rejection, 90% stroke.

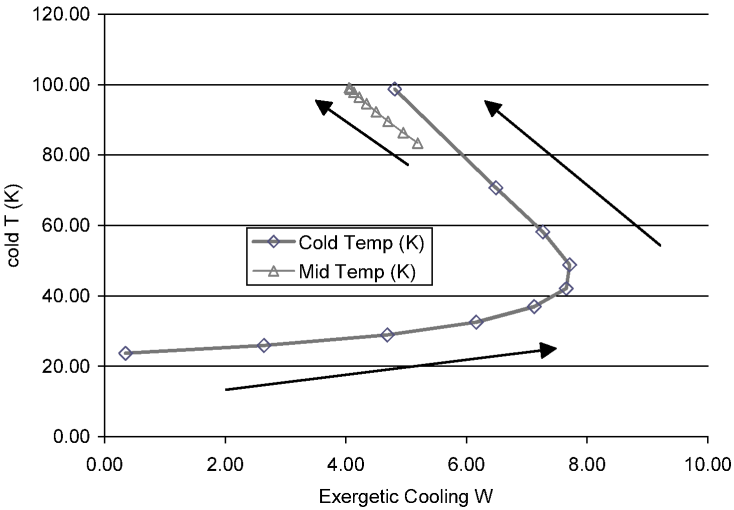


Figure 5. Exergetic cooling (from performance in Figure 2) paths.

change in loads could make both stages more inefficient. Figure 5 shows how the low stage cooling is maximized in the 40 K to 50 K range, whereas the high stage’s cooling monotonically decreases at a slowing rate in the measured range.

How Thermodynamic Systems Operate along Exergetic Paths

Any system’s approach to optimal operation is discussed in this proceedings¹ and in the prior literature². That discussion shows the theoretical basis for how a single stage refrigerator would operate along a looped path on the exergetic cooling versus exergetic efficiency plane. Inspection of Equations 1 and 2, along with a cursory knowledge of refrigeration systems shows why this is true for all multistaged systems as well. With no external cooling loads, the system cooling temperatures decline to their *no load* temperatures, at which state the system is operating in a non optimal manner. Given no load, exergetic efficiency and cooling are zero. As is demonstrated in Figure 6, increased exergetic cooling loads also increases efficiency, until exergetic efficiency is maximized. Beyond this maxima, the path turns downward until the maxima for exergetic cooling

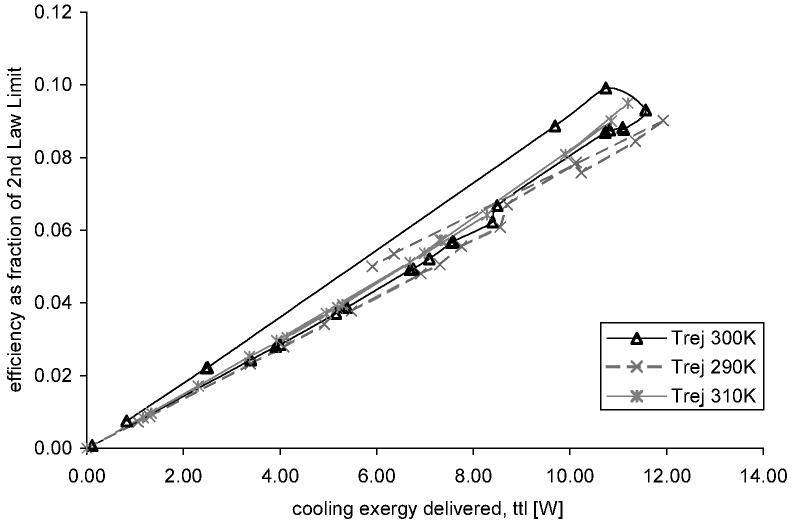


Figure 6. Efficiency as % of Second Law limit as a function of Exergetic cooling, for 300 K rejection, 90% stroke.

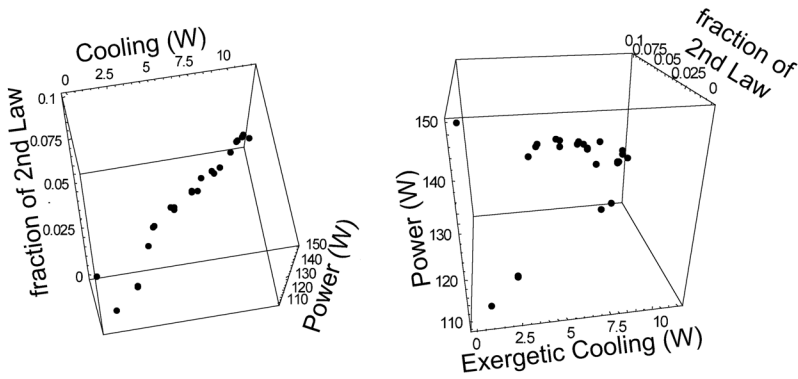


Figure 7a, b. 300 K rejection, 90% stroke exergetic cooling path.

is reached, and then the path turns back to the origin. The origin is reached again when both cooling temperatures equal the rejection temperature. This path is most clearly demonstrated in the 300 K data in Figure 6.

That path can be illuminated by its depiction for the 300 K data from Figure 6 and 7, in which the power input is used to show how the path follows a line in \mathbf{R}^3 . Figure 8 shows how rejection temperature effects both the power input requirement as well as creating another performance path for the system. What is clear from this type of thermodynamic path behavior is that just as a single stage refrigerator’s cooling capacity is distinctly determined by its environmental conditions and inputs, so is a multistage refrigerator.

A MODEL OF MULTISTAGE REFRIGERATION EMPIRICAL PERFORMANCE

At this point, it should be noted what progress has been made by recognition of these performance paths.

1. For a given stroke, it is no longer necessary to plot multitudinous graphical depictions of refrigeration performance; instead, the whole performance envelope fits on one graph.
2. Graphical comparison between coolers becomes easier for their entire performance envelope.
3. An explicit correlation of work input as a function of cooling temperatures, rejection tem-

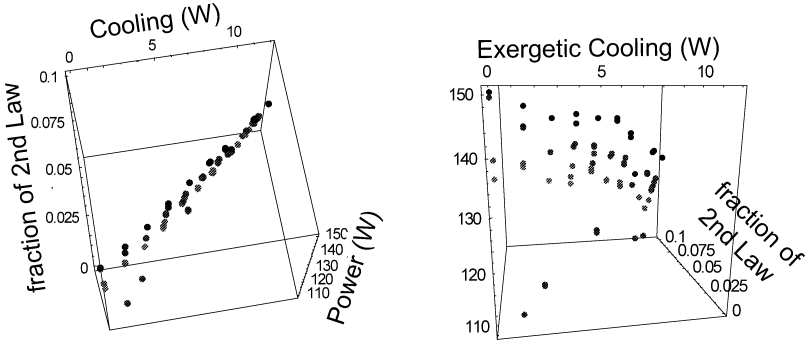


Figure 8a, b. 290-310 K rejection, 90% stroke actual exergetic cooling path.

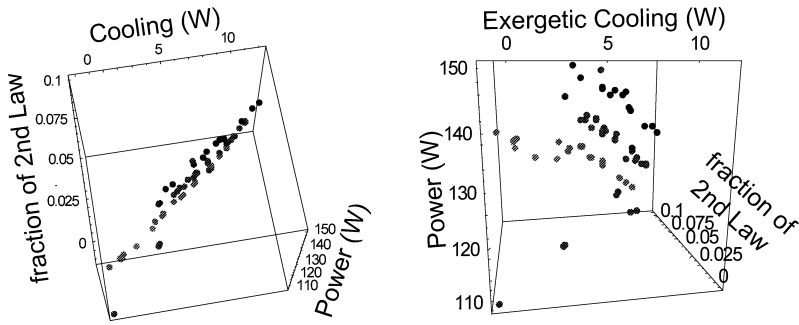


Figure 9a, b. 290-310 K rejection, 90% stroke model exergetic cooling path.

perature, and total exergetic cooling can be made. Presumably, such correlations would make numerical comparison of systems facile as well.

Razani¹ offers the single-stage estimate for exergetic efficiency:

$$\eta_{exer} = \frac{Q_{cooling,exerg}}{P_{input}} = \left(\frac{T_{rej}}{T_c} - 1\right) \left[Pr \frac{T_c}{T_{rej}} - \beta \left(\sqrt{1 + \alpha \left(\frac{1 + Pr}{1 - Pr}\right)^2} - \frac{T_c}{T_{rej}} \right) \right] \quad (3)$$

Assuming Eq. 3 can be understood for a multistage system using Eq. 1, Eq. 3 could be rewritten for the multistage refrigerator as:

$$\eta_{exer} = \frac{Q_{cooling,exerg}}{P_{input}} = C + \sum_{i=1}^n A_i \left(\frac{T_{c,i}}{T_{rej}} - 1 \right) - \frac{B_i}{P_{input}} \left(\frac{T_{rej}}{T_{c,i}} - 1 \right) \quad (4)$$

This estimate uses the coefficients A_i , B_i to encompass the effects of the internal processes for each stage discussed by Razani¹, and furthermore assumes that they are constant for all equilibrium states along the exergy path the system displays, such as those in Figures 6 through 8. This estimate

Table 1. Model Parameter Estimation

	Estimate	TStat
C	0.125848	2.72245
A_1	0.193853	8.76845
B_1	-0.148699	-1.60863
A_2	1.39742	11.1595
B_2	1.43531	1.75665

$R^2 = 0.868239$ Estimated Variance = 0.000115872

Subscripts 1,2 referring to low and high stages respectively

was correlated with the mapping data from the SB235 cooler with the statistical results found in Table 1 and the graphical results shown in Figure 9.

It should be noted that the assumption of the coefficients A_i , B_i being constant is possibly the reason behind the modest R^2 value of the regression analysis. Razani¹ developed Eq. 3 for optimal system performance, and by definition the many equilibrium states in the mapping data are not all optimal conditions. This analysis allows for the identification of which states are close to optimal. Such optimum would be indicative of the ranges about which a particular system could be used flexibly in response to unanticipated applications or missions.

CONCLUSIONS AND FUTURE WORK

The principal direction that this investigation will take in the future will be in determining how available work, and, therefore, how exergetic cooling is proportioned between stages as cooling loads and temperatures, as well as, power inputs and rejection temperatures vary. This estimate must take into account non-optimal performance states as is presented in these proceedings³. In addition, it is a virtual certainty that such proportioning is due principally to the geometry of the system, so therefore a summary knowledge of the internal construction of the system will be required. This does not imply that a detailed model of the internal component performance of the refrigerator is necessary, at the level of models that might be needed for specific system designs prior to fabrication.

Comparison of various refrigeration systems will be made between the Ball SB 235, NGST HCC, and Raytheon RS2P systems that will demonstrate the inherent performance differences between these multistage systems. It is anticipated that significant performance differences between Stirling-cycle system and its pulse tube variants will be numerically comparable using this exergy-based approach.

NOTATION

α	ratio of void volume of the regenerator, times frequency, divided by regenerator conductance ¹
β	non dimensional group expressing ratio of fill pressure to pressure amplitude delivered by compressor
η	efficiency
Q	cooling load
T	temperature
P	power
Pr	pressure amplitude drop across regenerator ¹

Subscripts

c	cooling
exer	exergetic
in	input
rej	rejection

REFERENCES

1. Razani, A. et al, "The Second Law Based Thermodynamic Optimization Criteria for Pulse Tube Refrigerators," *Cryocoolers 14*, ICC Press, Boulder, CO (2007), this proceedings.
2. Chen, J. et al, "On the Curzon-Ahlborn Efficiency and its Connection with the Efficiencies of Real Heat Engines," *Energy Conversion and Management*, Vol 42 (2001), pp. 173-181
3. Dodson, C. et al, "A Model for Parametric Analysis of Pulse Tube Losses in Pulse Tube Refrigerators," *Cryocoolers 14*, ICC Press, Boulder, CO (2007), this proceedings.